

Distribution Agreement

In presenting this thesis as a partial fulfillment of the requirements for a degree from Emory University, I hereby grant to Emory University and its agents the non-exclusive license to archive, make accessible, and display my thesis in whole or in part in all forms of media, now or hereafter now, including display on the World Wide Web. I understand that I may select some access restrictions as part of the online submission of this thesis. I retain all ownership rights to the copyright of the thesis. I also retain the right to use in future works (such as articles or books) all or part of this thesis.

Chandler H. Fountain

4/15/2012

**An Investigation of the Supercoiling Activities of *E. coli* and *Salmonella* Gyrases Using
Magnetic Tweezers**

by

Chandler H. Fountain

Dr. Laura Finzi, Ph.D.
Adviser

Department of Physics

Dr. Ivan Rasnik, Ph.D.
Committee Member

Dr. David D. Dunlap, Ph.D.
Committee Member

2012

**An Investigation of the Supercoiling Activities of *E. coli* and *Salmonella* Gyrases Using
Magnetic Tweezers**

By

Chandler Fountain

Dr. Laura Finzi, Ph.D.

Adviser

An abstract of
a thesis submitted to the Faculty of Emory College of Arts and Sciences
of Emory University in partial fulfillment
of the requirements of the degree of
Bachelor of Sciences with Honors

Department of Physics

2012

Abstract

An Investigation of the Supercoiling Activities of *E. coli* and *Salmonella* Gyrases Using Magnetic Tweezers

By Chandler Fountain

Eukaryotic and prokaryotic organisms possess members of the topoisomerase family of enzymes in order to regulate the level of DNA supercoiling throughout their life cycle. DNA supercoiling is regulated in a dynamic fashion and is known to play a role in the expression of genes, site-specific recombination, DNA condensation, and the segregation of chromosomes. K. Champion and N. P. Higgins showed that replacing the *gyrB* subunit of gyrase in *E. coli* with that of *Salmonella* resulted in death of the bacteria. The goal of this study was to explore the differences between *E. coli* gyrase and *Salmonella* gyrase using single molecule experiments. Magnetic tweezers were used to investigate the relative relaxation rates of (+) supercoils, frequency of pausing, duration of pausing, and relative introduction rates of (-) supercoils. It was found that *Salmonella* gyrase relaxed (+) supercoils at a slightly slower rate than *E. coli* gyrase. Furthermore, *Salmonella* gyrase was observed to pause for smaller durations, but at a higher frequency than *E. coli* gyrase. It was also found that *Salmonella* gyrase relaxed (-) supercoils at a higher rate than *E. coli* gyrase. Additionally, *Salmonella* gyrase introduced a slightly larger number of supercoils in each supercoiling event.

**An Investigation of the Supercoiling Activities of *E. coli* and *Salmonella* Gyrases Using
Magnetic Tweezers**

By

Chandler Fountain

Dr. Laura Finzi, Ph.D.

Adviser

A thesis submitted to the Faculty of Emory College of Arts and Sciences
of Emory University in partial fulfillment
of the requirements of the degree of
Bachelor of Sciences with Honors

Department of Physics

2012

Acknowledgements

I would like to thank both Dr. Finzi and Dr. Dunlap for their guidance and support throughout my time in the Finzi lab. Under their leadership, I have grown as both a researcher and as an individual. I would also like to thank Dr. Sachin Goyal for his teaching and kind words throughout my early months in the lab. From retrieving a hard-to-get DNA fragment to troubleshooting magnetic tweezers, my work with Dr. Goyal taught me the key to research is dedication and perseverance.

I am very grateful to fellow lab members Dr. Qing Shao, Yue Ding, Suleyman Ucuncuoglu, and Dr. Haowei Wang for their help with experiments and data analysis. A very special thanks is also due to Mónica Fernández Sierra. Her willingness to help with and her dedication to this project were inspirational and extraordinarily helpful. Fruitful discussions with Mónica were the basis for many ideas and breakthroughs that helped this project to progress as it has.

Finally, I would like to extend great thanks to my friends and family members who offered words of encouragement along the way.

TABLE OF CONTENTS

1. Introduction.....	1
1.1 Motivation	1
1.2 DNA and its interaction with protein.....	2
1.3 DNA Supercoiling – Terminology and importance	3
1.4 DNA Gyrase	5
1.5 Magnetic Tweezers.....	8
2. Materials and Methods.....	11
2.1 DNA Construct.....	11
2.1.1 Main Fragment (ApaI-NgoMIV Digest)	11
2.1.2 Main Fragment (XmaI-PciI Digest)	14
2.1.3 Tail Fragments (for the ApaI-NgoMIV Main Fragment)	15
2.1.4 Tail Fragments (for the XmaI-PciI Main Fragment).....	17
2.1.5 Ligation of Main Fragment and Tails.....	17
2.2 Magnetic Tweezers Chamber Preparation.....	18
2.3 Magnetic Tweezers Experiment.....	21
2.3.1 Chapeau curves for extension vs. turns.....	24
2.3.2 Force vs. extension curves for force values	25
2.3.3 Difference in two experiment styles	26
2.3.4 (+) Supercoil relaxation experiment	26
2.3.5 Force modulation experiment.....	30
3. Results.....	32
3.1 (+) Supercoil relaxation results.....	32
3.2 Force modulated activity of gyrase.....	36
4. Discussion.....	39
5. Conclusion	46
Appendix.....	48
A1 Plot Trace File.....	48
A2 Rate Calibration	48
Bibliography	49

List of Figures

Figure 1.1: (A) Gene map with primary domains in different colors for three representative type IIA Topoisomerases (b) <i>S. Cerevisiae</i> gyrase structure with colored domains (<i>E. coli</i> gyrase in inset). The C-terminal domain is not shown. [11]	6
Figure 1.2: (A) model of Type IIA Topoisomerase (B) Reaction mechanism: G-segment binds to dna gate (step 1). T-segment captured after binding of ATP (step 2). hydrolysis of ATP and release of P_i causes DNA gate to open for strand passage (step 3). Remaining hydrolysis products released while G-segment is religated, T-segment is released, and ATP gate is reset (step 4). [13]	7
Figure 1.3: Magnetic tweezer setup	9
Figure 1.4: Manipulation of tension and twist on a DNA molecule using magnetic tweezers	9
Figure 2.1: A Plasmid map of pUC18-nuB104 showing the primers used to amplify the ApaI-NgoMIV main fragment	12
Figure 2.2: Restriction digest map of the plasmid pUC18-nuB104 used to produce the XmaI-PciI main fragment	14
Figure 2.3: Magnetic tweezers chamber	19
Figure 2.4: Magnetic tweezers instrument	22
Figure 2.5: Low force chapeau curve	24
Figure 2.6: High force chapeau curve	25
Figure 2.7: Example trace for (+) relaxation	29
Figure 3.1: Relaxation rates for <i>E. coli</i> gyrase vs. <i>Salmonella</i> gyrase. (a) Raw data points with mean and standard deviation bars. (b) Box and whisker plots showing sample minimum, lower quartile, median, upper quartile, and sample maximum.	34
Figure 3.2: Number of pauses observed per relaxation event.....	35
Figure 3.3: Cumulative distribution of the duration of pauses for (+) supercoil relaxation by <i>E. coli</i> and <i>Salmonella</i> gyrase	36
Figure 3.4: Rates of introduction of (-) supercoils by <i>E. coli</i> and <i>Salmonella</i> gyrase. (a) Raw data points with mean and standard deviation bars. (b) Box and whisker plots showing sample minimum, lower quartile, median, upper quartile, and sample maximum.	37
Figure 3.5: Number of (-) turns introduced by <i>E. coli</i> and <i>Salmonella</i> gyrases in each complete supercoiling event. (a) Raw data points with mean and standard deviation bars. (b) Box and whisker plots showing sample minimum, lower quartile, median, upper quartile, and sample maximum.....	38

Figure 4.1: Amino acid sequence alignment of *gyrA*. Light gray represents dissimilarities, red represents negatively charged residues, and green represents positively charged residues..... 42

Figure 4.2: Amino acid sequence alignment of *gyrB*. Light gray represents dissimilarities, red represents negatively charged residues, and green represents positively charged residues..... 43

List of Tables

Table 2.1: PCR protocol for main fragment.....	13
Table 2.2: Main fragment double digestion	14
Table 2.3: PCR protocol for biotin labeled tail.....	16
Table 2.4: PCR protocol for digoxigenin labeled tail.....	16
Table 2.5: Main fragment and tail ligation protocol.....	18
Table 2.6: Buffers and chemicals for MT chamber preparation.....	18

1. INTRODUCTION

1.1 MOTIVATION

The motivation for this study comes from the comparison of *E. coli* and *Salmonella* gyrases using bulk measurements by Champion, K. and Higgins, N. P. [1]. Champion and Higgins showed that during growth in rich medium, *E. coli* gyrase generates 15% more negative supercoils *Salmonella* gyrase. Furthermore, the average supercoil density for *Salmonella* is 13% less than that for *E. coli*. It is proposed that the difference in supercoiling behavior arises from gyrase's response to different levels of DNA strain. To investigate the behavior of the two gyrases further, Professor Higgins delivered *E. coli* and *Salmonella* gyrases to our lab for use in single molecule experiments. The main protocol of experiment involved adding positive (+) supercoils to a DNA segment at 0.6pN of force and allowing gyrase to relax the supercoils. For a fixed level of DNA strain, differences in the (+) supercoil relaxation behavior of the two enzymes were expected.

While collecting data with the style of experiment mentioned above, a second style of experiment became of interest after reviewing Nollman's 2007 article on the multiple modes of *E. coli* gyrase [2]. In this article, the activity of gyrase was modulated by force; the two modes are ATP-dependent introduction of (-) supercoils at low force (0.4pN) and ATP-independent relaxation of (-) supercoils at high force (0.7pN). This style of experiment was conducted using both *E. coli* and *Salmonella* gyrases. Extending this idea, it was thought that an intermediate force

value where gyrase dynamically switched between the two modes could be found. Given the postulation by Higgins that gyrase's activity is related to the level of DNA strain, the exact value of this "intermediate" force might differ for *E. coli* and *Salmonella* gyrases.

1.2 DNA AND ITS INTERACTION WITH PROTEIN

The genetic basis of all living organisms from single-celled bacteria to human beings is DNA, a key molecule of the cell that consists of two antiparallel strands of nucleotides. Each nucleotide consists of a nucleobase, a five-carbon sugar, and a phosphate group. Four different bases give rise to the four different nucleotides that comprise DNA: adenine (A), thymine (T), guanine (G), and cytosine (C). For RNA, uracil (U) replaces thymine. These nucleotides link to one other through phosphodiester bonds between the phosphate and sugar of adjacent nucleotides. The result is a single-stranded DNA molecule (sDNA) with a sugar-phosphate backbone. Two sDNA molecules can align antiparallel to form a double stranded DNA molecule (dsDNA) [3]. It was first proposed in 1953 by Watson and Crick that the secondary structure of DNA was that of a double helix [4]. The dsDNA double helix is stabilized by hydrogen bonds (H-bonds) between complimentary nucleobases known as base pairs (bp). G pairs with C through three H-bonds, while A pairs with T through two H-bonds. Specific DNA sequences code for specific proteins, and these proteins perform a multitude of biochemically important functions [3].

DNA-protein interactions play a role in cellular metabolism, development, and replication. Proteins can interact specifically and non-specifically with DNA. A specific interaction is a site-specific interaction that depends on the DNA base pair sequence [5]. Of particular interest to our study are the protein-DNA interactions that help a cell to maintain a relatively constant level of supercoiling, which establishes the tertiary structure of DNA. DNA from different cellular sources have a unique degree of supercoiling that is characteristic of the organism [3]. Supercoiling and the associated terminology will be discussed next, followed by a description of the class of enzymes that work to introduce and relax supercoils.

1.3 DNA SUPERCOILING – TERMINOLOGY AND IMPORTANCE

Under normal cellular conditions, DNA intrinsically forms tangles without any applied torsion. Proteins further modify DNA topology for compaction and storage. For cellular processes in which the DNA base sequence must be accessed, proteins act on DNA to relax it from its compacted form. The number of times the DNA double helix crosses over itself is known as the linking number (Lk). Linking number is a topological property that can only be changed by breaking one or both strands of the DNA backbone. Twist (Tw) and writhe (Wr) are two geometric parameters of DNA that can alter the linking number. Twist describes the helical winding of DNA strands around one another, while writhe describes the coiling of the DNA axis around itself [6]. Linking number is related to twist and writhe by the equation

$$Lk = Tw + Wr \quad . \quad (1)$$

For torsionally relaxed B-DNA, the twist (Tw_0) is one turn every 10.4 bp and the writhe (Wr_0) is zero. When over-wound or under-wound relative to this relaxed form, the linking number changes. The excess linking number or supercoil density, σ , is defined as

$$\sigma = \frac{Lk - Lk_0}{Lk_0} . \quad (2)$$

Over-wound DNA gives a positive σ , while under wound DNA gives a negative σ [7]. To relieve twisting strain on the DNA molecule, writhe may form in order to maintain linking number. Writhe can take the form of plectonemes or solenoids. Of particular interest to our study are plectonemes, which are extruded intertwined loops [6]. Linking number can be changed experimentally, but is also constantly changing in local segments of DNA in every living cell.

DNA topology is altered in a number of cellular processes including DNA replication, transcription, and DNA recombination. The addition of supercoils to DNA is best visualized for a constrained piece of DNA, either a loop or a segment fixed at both ends to membranes or the cytoskeleton. In the cellular processes mentioned above, dsDNA must progressively untwist, so that ssDNA nucleotides can be accessed by transcription and replication machinery. This unwinding of DNA causes the over winding of DNA ahead of the machinery and under winding behind the machinery. This over and under winding is relative to the characteristic level of supercoiling in individual organisms [8]. Just as these processes affect the level of supercoiling, the inverse is true; the level of supercoiling determines whether or not these processes can happen. The level of supercoiling is known to play a role in the

expression of genes, site specific recombination, DNA condensation, and segregation of chromosomes. To maintain a particular level of supercoiling, cells rely on proteins in the topoisomerase family.

In bacteria, the level of supercoiling is maintained by four enzymes known as topoisomerases. Topoisomerase I and topoisomerase III are type I topoisomerases that effectively transfer one single-stranded filament of a dsDNA molecule through the antiparallel filament to decrease the twist linking number in steps of one. DNA gyrase and topoisomerase IV are type II topoisomerases that make double stranded breaks in DNA to decrease the linking number in steps of two. It has been shown that the removal of any one of these enzymes alters the level of supercoiling in the cell [9]. The mechanism of each enzyme is intriguing, but the mechanism of DNA gyrase is of particular interest to our study.

1.4 DNA GYRASE

There are many types of type IIA topoisomerases, but only the structure and mechanism of bacterial topo IIA (or gyrase) will be covered here. Gyrase is an A₂B₂ heterotetramer of the two subunits *gyrA* and *gyrB*. The enzyme works to pass a dsDNA transfer segment (T-segment) through a cleaved dsDNA gate segment (G-segment). As seen in Figure 1, *gyrB* encodes the ATPase domain (of the GHKL¹ family), the transducer domain, and the metal-binding TOPRIM domain; *gyrA* encodes the winged helix domain (WHD), the tower domain, the coiled-coil domain,

¹ Gyrase, Heat-shock protein 90, histidine Kinase, and MukL – a family of ATPases

² Also known as the 5Y-CAP because of a catalytic tyrosine residue that attacks the 5

and the C-terminal domain [10]. These domains are arranged in such a way that gyrase can hold a cleaved dsDNA segment while another dsDNA segment is passed through it.

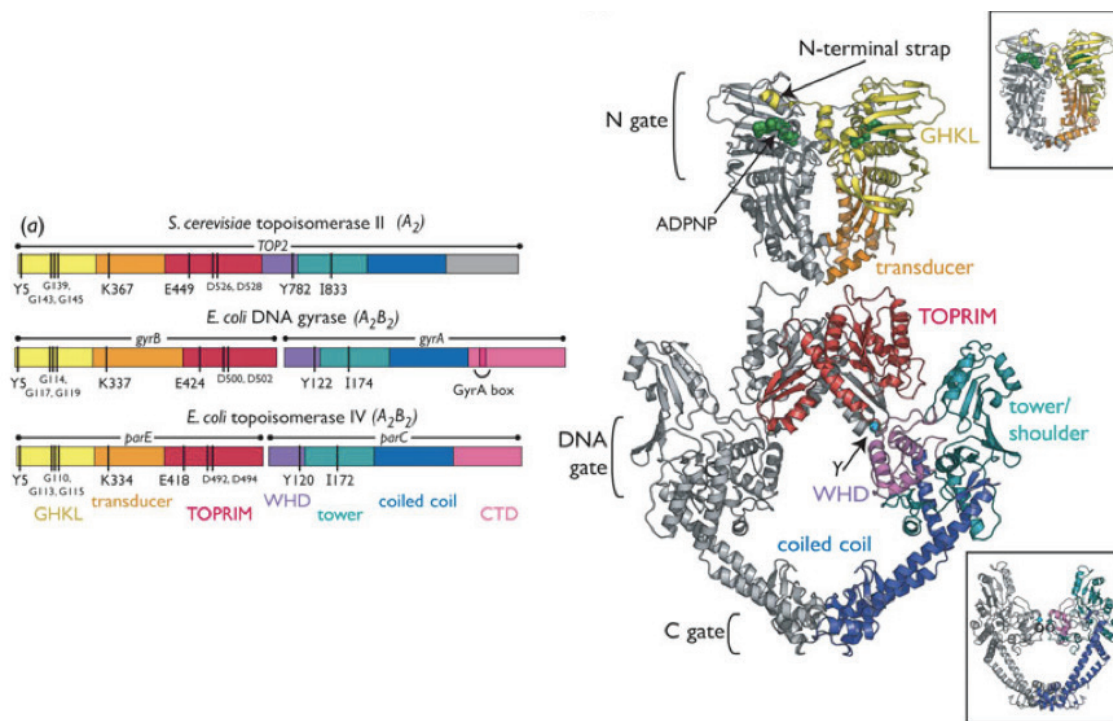


Figure 1.1: (A) Gene map with primary domains in different colors for three representative type IIa Topoisomerases (b) *S. Cerevisiae* gyrase structure with colored domains (*E. coli* gyrase in inset). The C-terminal domain is not shown. [11]

The mechanism of gyrase seems to depend on the arrangement of the aforementioned domains into three gates. The first gate, the N-gate, is the entry gate for the T-segment and is formed by the ATPase and transducer domain. The transducer domain links the N-gate to the second gate, the central gate, which is

formed by the WHD (5Y-CAP²) and the TOPRIM domain; the G-segment is bound by these domains and cleaved³ [12]. The third gate is the C-gate, which is formed by the coiled-coiled domain. The three gates of gyrase open and close at different points during the reaction cycle [13].

Gyrase employs a multistep mechanism in order to pass one dsDNA through another (Figure 1.2). The reaction begins with the binding of the G-segment. The T-segment is then captured upon ATP-induced dimerization of the ATPase domains of the N-gate. Next, the G-segment is cleaved and the T-segment is passed through. After T-segment passage, the G-segment is religated and the C-gate opens to allow release of the T-segment. Release of ADP resets the N-gate to its open formation and prepares the enzyme for another cycle.

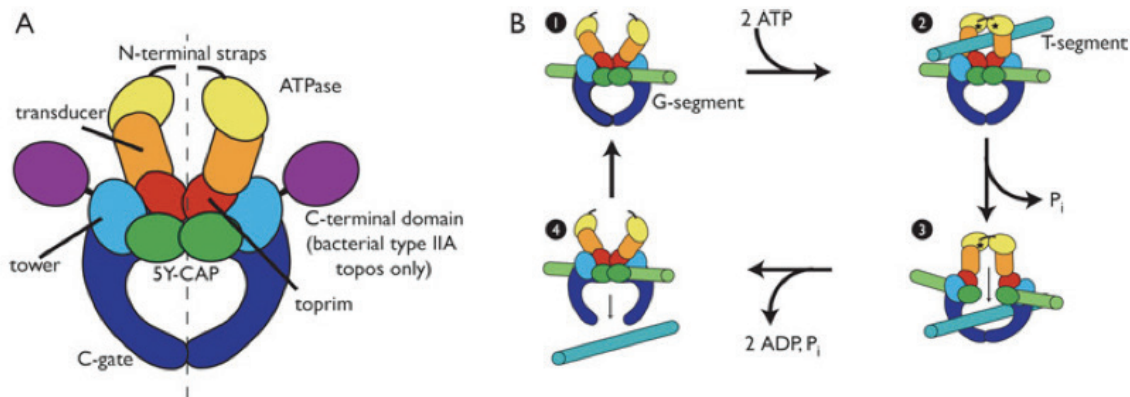


Figure 1.2: (A) model of Type IIA Topoisomerase (B) Reaction mechanism: G-segment binds to dna gate (step 1). T-segment captured after binding of ATP (step 2). hydrolysis of ATP and

² Also known as the 5Y-CAP because of a catalytic tyrosine residue that attacks the 5 end of DNA [11].

³ Cleavage is thought to be made possible by the positioning acidic residues in the TOPRIM domain close to the catalytic tyrosine of the 5Y-CAP [11]

release of P_i causes DNA gate to open for strand passage (step 3). Remaining hydrolysis products released while G-segment is religated, T-segment is released, and ATP gate is reset (step 4). [13]

The studies of type IIA topoisomerases have led to recent advances that give more insight into the exact timing of ATP hydrolysis [11] and the role of the C-terminal domain, which is known to wrap 128-140 bp of DNA [14, 15]. Some of the most enlightening of these studies are single molecule studies, which employ optical tweezers, magnetic tweezers, and atomic force microscopy experiments [16]. In this study, magnetic tweezers were used to manipulate the supercoiling level of a single DNA molecule in the presence of gyrase.

1.5 MAGNETIC TWEEZERS

Magnetic tweezers are a single molecule manipulation technique that allows the experimenter to manipulate and monitor a single DNA molecule. A paramagnetic bead attached to one end of the DNA strand allows for adjustment of the force applied to the molecule and the coiling level of the molecule. Magnetic tweezers have been used to study different aspects of type IIA topoisomerase, such as the reaction mechanism and the force-sensitivity [17, 18]. Magnetic tweezers consist of a pair of permanent magnets under computer control positioned above a flow chamber (Figure 1.3).

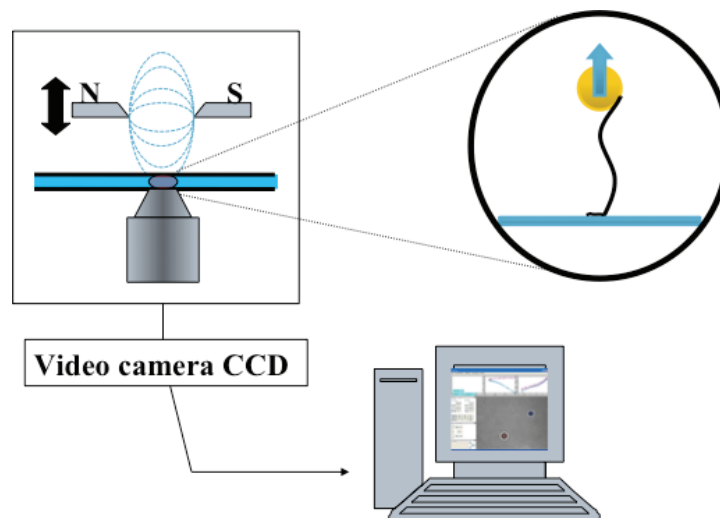


Figure 1.3: Magnetic tweezer setup

The flow chamber is positioned on a stage which can be translated in the x and y directions. Inside the chamber are DNA molecules tethered to the bottom surface at one end and to a paramagnetic bead at the other end. This allows for stretching (in the z -direction) or positive or negative twisting of the molecule (Figure 1.4).

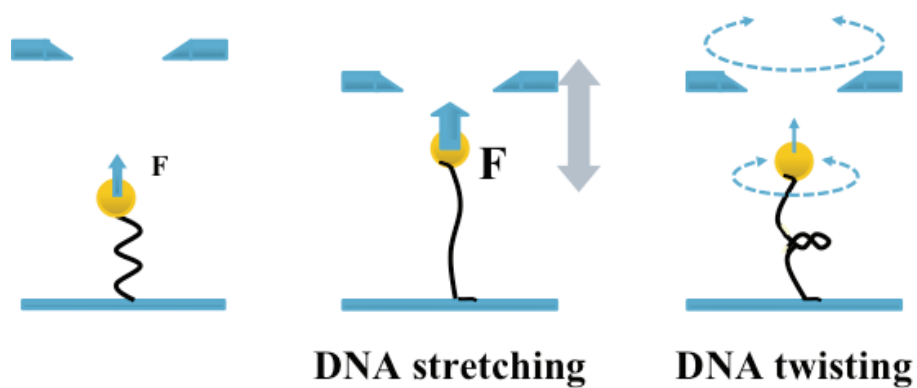


Figure 1.4: Manipulation of tension and twist on a DNA molecule using magnetic tweezers

The chamber sits atop an inverted objective lens that focuses LED light from above onto a CCD camera. The video is displayed in the same Matlab applet that is used to control the pair of magnets. Interference between the unscattered LED light and light scattered off the paramagnetic beads gives a diffraction pattern of concentric rings around the bead. These concentric rings change as the distance between the bead and the focal point of the objective lens changes.

As a calibration with which to determine the length of the DNA tether, a piezoelectric motor changed the position of the objective in steps of $0.2\mu\text{m}$ and recorded the diffraction pattern at each step. This calibration was used to compare the diffraction pattern of a reference bead on the glass surface to the diffraction pattern of the DNA-tethered bead to give the length of the DNA tether. The Brownian motion of the bead was recorded and used to calculate the force on the molecule using the equation

$$F = \frac{k_B T l}{\delta x^2} . \quad (3)$$

where k_B is Boltzmann's constant, T is temperature, l is the length of the DNA molecule, and δx^2 is the mean square of the bead's fluctuation in the x-direction [16]. The extension of the DNA molecule can be measured as a function of force or the number of turns added to the DNA. Furthermore, the extension of the DNA molecule can be monitored as a function of time. This is particularly useful for monitoring DNA extension changes due to enzyme activity.

2. MATERIALS AND METHODS

2.1 DNA CONSTRUCT

The DNA fragment introduced into the flow chamber consists of a main fragment, a biotin- (bio) labeled tail, and a digoxigenin- (dig) labeled tail. The fragments are attached to one another by digesting with restriction endonucleases and then ligating complimentary overhangs. First, a double digestion is performed with two different restriction enzymes on the main fragment. Next, the biotin- and digoxigenin-labeled tails were digested with one of the two restriction enzymes used to digest the main fragment. Finally, the three fragments were ligated using T4 DNA Ligase, resulting in the desired DNA construct. The biotin-labeled tail binds to a paramagnetic bead, which is coated with streptavidin. The digoxigenin-labeled tail binds to the surface, which is coated in digoxigenin's antibody, anti-digoxigenin (anti-dig). Multiple binding sites on the two tail fragments prohibit the DNA tether from freely rotating, as it would with only a single binding site at each end.

2.1.1 MAIN FRAGMENT (APAI-NGOMIV DIGEST)

The main fragment of DNA was produced from pUC18-nuB104 plasmid provided by N. Patrick Higgins of the University of Alabama at Birmingham (UAB). Stocks of the plasmid were prepared and frozen by Sharon Owino, a previous lab member. Sharon conducted trials with different reaction conditions; the reaction with the best yield was used. These stocks were thawed when needed. Figure 2.1 shows a map of the plasmid. Since pUC18-nuB104 has few useful restriction sites with

complimentary overhangs to those of labeled tails produced using pBLuKSP, primers containing restriction sites were used to amplify the main segment.

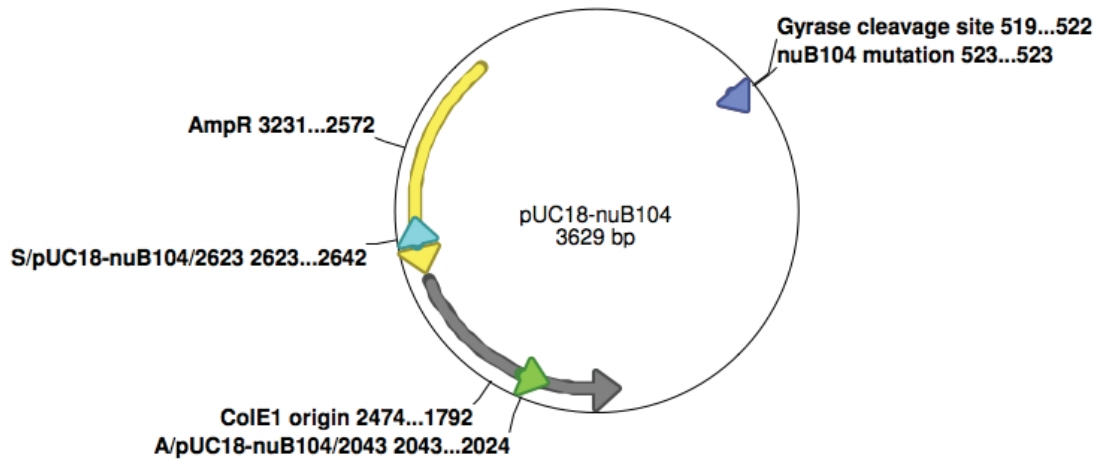


Figure 2.1: A Plasmid map of pUC18-nuB104 showing the primers used to amplify the ApaI-NgoMIV main fragment

Polymerase chain reaction (PCR) was used to amplify the desired region using the sense primer S/pUC18-nuB104/2623-NgoMIV and the antisense primer A/pUC18-nuB104/2043-ApaI. Primers are small segments of DNA that are complimentary to short sequences that define each end of the desired DNA fragment. PCR consists of a number of steps. First, the temperature is raised to denature the dsDNA template. Second, the temperature is lowered to allow the primers to anneal. Third, the temperature is raised again to allow Taq Polymerase (New England Biolabs, Ipswich, MA) to polymerize the complimentary DNA strand using free nucleotides, dATPs, dTTPs, dCTPs, and dGTPs (collectively known as dNTPs; Fermentas, Glen Burnie, Maryland), that are added to the reaction solution.

This process is repeated for ~30 cycles to produce many copies of the 3065 bp DNA fragment of interest. The PCR protocol can be found in Table 2.1.

Table 2.1: PCR protocol for main fragment

	label		1 to 6		
	PCR volume (ul)	30	bp	master mix	0.04 extra
H2O			24.93	149.58	155.56
LongAmp Taq Buffer	10	X	2.00	12.00	12.48
LongAmp Taq	5	U/ul	0.40	2.40	2.50
dNTP Mix (Fermentas)	10	mM	0.60	3.60	3.74
2 S/pUC18-nuB104/2623-NgoMIV(tm=54.1)	10	U/ul	1.00	6.00	6.24
6 A/pUC18-nuB104/2043-Apa1(tm=55.8)	10	mM	1.00	6.00	6.24
pUC18-nuB104	150	mM	0.07	0.42	0.44
total (ul)			30.00	180.00	187.20
	volume from master mix		30.00	residue	7.20
		time	Temp (degrees)		
	initial denaturation (min)	1:00	95		
	denaturation time (min)	0:05	94		
	annealing time (min)	0:05	56		
	elongation time (min)	2:05	68		
	number of cycles	30			
	finishing elongation (min)	4:00	68		
	re-annealing (min)	5:00	55		
	re-annealing (min)	3:00	37		
	forever		4		

The PCR product was cleaned up using a Qiagen PCR Cleanup Kit according to the instructions included with the kit. The next step was to perform a double digestion of the PCR product (Table 2.2). ApaI and NgoMIV were used for the digestion because the S/pUC18-nuB104/2623-NgoMIV primer contained an NgoMIV restriction site and the A/pUC18-nuB104/ApaI primer contained an ApaI restriction site. The digestion product was cleaned up with a PCR Cleanup Kit (Qiagen). The resulting fragment was 3065 bp long with ApaI and NgoMIV overhangs.

Table 2.2: Main fragment double digestion

	concentration	volume [ul]
H2O		5.44
Buffer 4	10X	5.0
BSA	100X	0.5
pUC18-nuB104	125 ng/ml	38.1
NgoMIV (no BSA)	10 U/ul	0.48
Apal	10 U/ul	0.48
total		50

2.1.2 MAIN FRAGMENT (XMAI-PCII DIGEST)

An alternate segment of the main fragment was initially used because of availability. This fragment was obtained by direct digestion with XmaI and PciI restriction enzymes (NEB) (Figure 2.2). The resulting fragment after digestion and cleanup was 3165 bp, 100 bp longer than the Apal-NgoMIV main fragment.

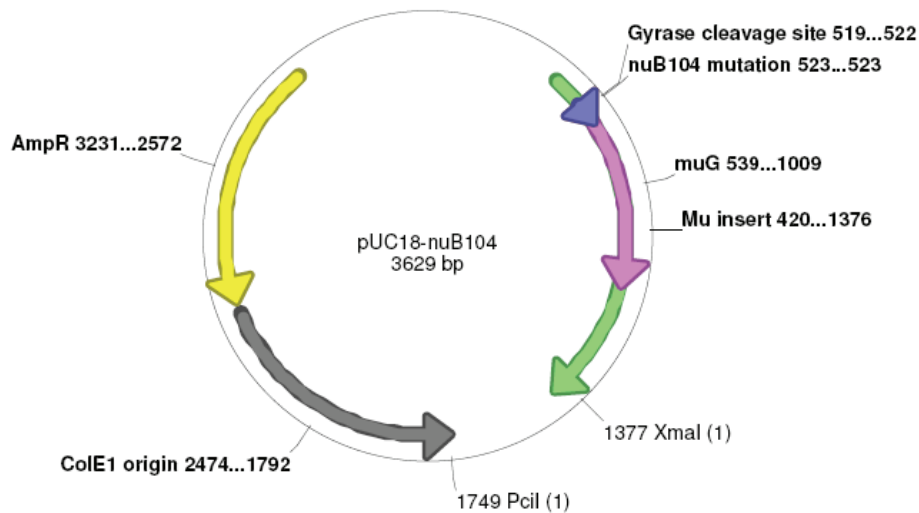


Figure 2.2: Restriction digest map of the plasmid pUC18-nuB104 used to produce the XmaI-PciI main fragment

Due to the low yield of this fragment, it was abandoned and the higher yield ApaI-NgoMIV main fragment was used.

2.1.3 TAIL FRAGMENTS (FOR THE APAI-NGOMIV MAIN FRAGMENT)

In addition to producing the main fragment, Sharon Owino tested two plasmid templates, pUC19 and pBluKSP, for creating tail fragments via PCR and left amplicons in the lab freezer. The pBluKSP amplicons were used as tails for the ApaI-NgoMIV main fragment and the pUC19 stocks were used as tails for the XmaI-PciI main fragment. Sharon prepared the plasmid stocks using PCR to amplifying the region of interest. The primers S/pUC19/2412 and A/pUC19/1435 were used for pBluKSP. Two sets of PCR reactions were run, one for biotin-labeling and another for digoxigenin-labeling. As mentioned previously, biotin and digoxigenin labeling were carried out using bio-dUT (Fermentas, Glen Burnie, Maryland) and dig-UTP (Roche Applied Science, Indianapolis, IN) in addition to normal dNTP. The PCR protocol for these thermocycling reactions can be found in Table 2.3 and Table 2.4. The PCR products were purified using a PCR Cleanup Kit (Qiagen).

Table 2.3: PCR protocol for biotin labeled tail

	label	bio	bK1-8		
PCR volume (ul)		30			0.04
			bp	master mix	extra
H2O			20.13	161.04	167.48
Taq polymerase bfr (NEB)	10	X	3.00	24.00	24.96
pBluKSP	208	ng/ul	0.05	0.40	0.42
Taq Polymerase (NEB)	5	U/ul	0.50	4.00	4.16
dATP mix (Fermentas)	6	mM	1.00	8.00	8.32
dCTP mix (Fermentas)	6	mM	1.00	8.00	8.32
dGTP mix (Fermentas)	6	mM	1.00	8.00	8.32
dTTP mix (Fermentas)	6	mM	0.94	7.52	7.82
S/pUC19/2412 (Tm = 63)	10	uM	1.00	8.00	8.32
A/pUC19/1435(Tm = 55)	10	uM	1.00	8.00	8.32
bio-11-dUTP	1	mM	0.38	3.04	3.16
total (ul)			30.00	240.00	249.60
		volume from master mix	30.00	residue	129.60
initial denaturation (min)	1:00		95		
denaturation time (min)	0:05		94		
annealing time (min)	0:05		59		
elongation time (min)	2:05		72		
number of cycles	30				
finishing elongation (min)	4:00		72		
re-annealing (min)	5:00		55		
re-annealing (min)	3:00		37		
	forever		4		

Table 2.4: PCR protocol for digoxigenin labeled tail

	label	dig	dK1-8		
PCR volume (ul)		30			0.04
			bp	master mix	extra
H2O			20.13	161.04	167.48
Taq polymerase bfr (NEB)	10	X	3.00	24.00	24.96
pBluKSP	208	ng/ul	0.05	0.40	0.42
Taq Polymerase (NEB)	5	U/ul	0.50	4.00	4.16
dATP mix (Fermentas)	6	mM	1.00	8.00	8.32
dCTP mix (Fermentas)	6	mM	1.00	8.00	8.32
dGTP mix (Fermentas)	6	mM	1.00	8.00	8.32
dTTP mix (Fermentas)	6	mM	0.94	7.52	7.82
S/pUC19/2412 (Tm = 63)	10	uM	1.00	8.00	8.32
A/pUC19/1435(Tm = 55)	10	uM	1.00	8.00	8.32
dig-11-dUTP	1	mM	0.38	3.04	3.16
total (ul)			30.00	240.00	249.60
		volume from master mix	30.00	residue	129.60
PCR cycle Same as (Table 2.3)					

The bio-labeled pBluKSP was digested with *Apal* (NEB) and the digoxigenin-labeled pBluKSP fragment was digested with *XmaI* (NEB). These two restriction enzymes were chosen so that the 1 kbp biotin-labeled or digoxigenin-labeled fragments would have a complimentary overhang to opposite ends of the main fragment. *Apal* was an obvious choice since the same enzyme was used to cut one end of the main segment. *XmaI* was chosen because although the pBluKSP plasmid lacks an NgoMIV site, *XmaI* and NgoMIV have complementary 5'-CCGG overhangs.

2.1.4 TAIL FRAGMENTS (FOR THE XMAI-PCII MAIN FRAGMENT)

Using two different primer sets, Sharon Owino amplified biotin- and digoxigenin-labeled 2 kb regions of the pUC19 plasmid for ligation to the *XmaI*-*PciI* main fragment. The biotin-labeled fragment was digested with *XmaI* (NEB) and the digoxigenin-labeled fragment was digested with *PciI* (NEB) to produce tail segments with complimentary overhangs that were ligated to the 3165 bp main fragment.

2.1.5 LIGATION OF MAIN FRAGMENT AND TAILS

After digestion, the main fragment and tails were ready for ligation. The ligation reaction was a simple reaction in which tails and main fragments, in a four to one ratio, were added to a reaction mixture containing T4 DNA ligase in the manufacturer-supplied T4 DNA ligase buffer, and water. The reaction was left for three hours at room temperature or overnight at 16° C. Denaturing the T4 DNA ligase halts the ligation reaction. This was achieved by placing the reaction tube at 65° C for ten minutes; a PCR machine was used for convenience. After halting the

reaction, the mixture was stored at 4° C. A sample ligation protocol follows in Table 2.5. Without further purification, the DNA construct was ready for use in magnetic tweezers chambers.

Table 2.5: Main fragment and tail ligation protocol

ligation reaction volume (ul) =	30						
average MW/bp (g/mol/bp) =	650						
termini molar ratio =	3						
assumed ligation efficiency =	30						
desired amount of ligation (ng) =	150						
	length (bp)	MW	conc. (ng/ul)	conc. (nM)	pmol to mix	ng to mix	volume (ul)
main fragment (pUC18_nuB104)	3050	1982500	195	0.098	0.152	302.0	1.5
biotin tail fragment (ApaI)	1000	650000	36	0.055	0.457	297.0	8.3
digoxigenin tail fragment (XmaI)	1000	650000	43	0.066	0.457	297.0	6.9
reaction mix							
main DNA	1.5						
bio tail DNA	8.3						
dig tail DNA	6.9						
10x T4 DNA ligase buffer	3.0						
T4 DNA ligase (10 U/ul)	1.0						
H2O	9.3						
	30.0						

2.2 MAGNETIC TWEEZERS CHAMBER PREPARATION

Chambers for magnetic tweezers were made according to a protocol adapted from protocols belonging to fellow lab members Qing Shao and Yue Ding. The buffers and chemicals needed for sample preparation are listed in Table 2.6. A description of the protocol for a single chamber follows.

Table 2.6: Buffers and chemicals for MT chamber preparation

Buffer or Chemical	Composition
1X Phosphate-buffered saline (PBS)	Diluted from 10X PBS solution
20 $\mu\text{g}/\text{mL}$ Anti-digoxigenin	Diluted from 200 $\mu\text{g}/\text{mL}$ aliquots
λ buffer	10 mM Tris-HCl, , 0.1 mM EDTA, 20 mM KCl, 5% DMSO, 0.2 mM DTT, 0.5 mg/ml α -casein, pH 7.4
1X BSA	Diluted from NEB 100X BSA
Topo II buffer	50 mM Tris-HCl, 50 mM KCl, 8 mM MgCl_2 , 1 mM EDTA, 0.5 mM DTT, pH 7.9

The process began by making the physical chamber (Figure 2.3). Two glass cover slips were washed with 100% ethanol and placed on clean kimwipes. The slides were wiped gently with the kimwipes before the ethanol had evaporated. Two strips of double sided tape were cut and placed on the edges of the first cover slip. The shape of the chamber was defined by vacuum grease that was dispensed by a syringe. The second cover slip was then placed on the top. A optional thin line of grease could be applied across the top cover slip to prevent fluid from flowing across the top of the chamber. In Figure 2.3, the direction of flow was from top to bottom.

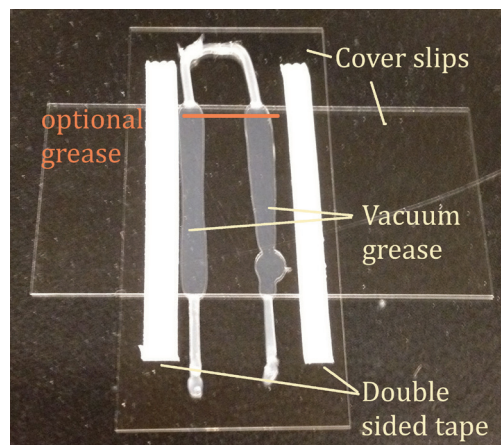


Figure 2.3: Magnetic tweezers chamber

After preparing the chambers, DNA and magnetic beads were introduced. 0.2 μL of Invitrogen MyOne (1 μm) beads were added to 200 μL 1X phosphate-buffered saline (PBS) in a 1.5 mL microcentrifuge tube. This tube was then placed in a magnetic tube stand to draw the beads to the side of the tube. The PBS was pipetted away carefully, leaving the beads on the side of the tube. The beads were re-suspended in 100 μL 1X PBS and placed in the magnetic tube stand again. The PBS was pipetted away a final time and the beads were re-suspended in 85 μL 1X PBS. This final solution was added to the dry chamber and flowed through by using a twisted kimwipe to draw away solution at the opposite end of the chamber. The chamber was allowed to sit for five minutes. These beads are introduced to serve as reference beads, which are beads fixed to the surface of the glass slide.

After five minutes, the chamber was washed with 200 μL 1X pBS. 100 μL of 20 $\mu\text{g}/\text{mL}$ anti-digoxigenin was then flowed in. As mentioned previously, anti-digoxigenin is the antibody to the digoxigenin label found on one tail of the DNA construct. In order to make sure the surface was coated thoroughly, the chamber was left in a humidity box overnight at 4° C. The humidity box was constructed from an unused pipette tip box. A kimwipe was put in the bottom of the box and enough distilled water was added to soak the kimwipe. The chamber was placed in the humidity box to prevent as much evaporation as possible.

The following morning, the chamber was washed with 800 μL of 1X PBS. After this wash, 100 μL of 1X BSA was flowed into the chamber and the chamber was

incubated again at 4° C in the humidity box for at least one hour. It was found that chambers at this step could be left for up to one day without ill effects. After at least one hour, the chamber was washed with 800 µL of λ buffer. Simultaneously, beads were washed according to the same procedure of suspending in 1X PBS and then using a magnetic tube stand to draw the beads to the side of the tube. This time however, the beads were washed in 200 µL of 1X PBS, 100 µL of 1X PBS, and then re-suspended in 10 µL of 1X PBS. 2 µL of the ligation product from section 2.1.5 was added to this bead solution and left to stand for five minutes. After five minutes, 85µL of λ buffer was added to the bead-DNA solution and mixed gently. At this point the bead-DNA solution was introduced into the chamber. The chamber was incubated for 45 minutes in the humidity box at 4° C prior to experimentation.

2.3 MAGNETIC TWEEZERS EXPERIMENT

The chamber was removed from the refrigerator and wiped gently with a kimwipe to remove any condensation from the humidity box. The chamber was inverted and a small drop of immersion oil was put on the chamber. The chamber was quickly flipped back over and placed on the stage of the magnetic tweezers instrument (Figure 2.4). Clips were used to hold the chamber in place for the duration of the experiment. At this point the LED light was turned on and the MATLAB code was run that opens the applet used to control the instrument.

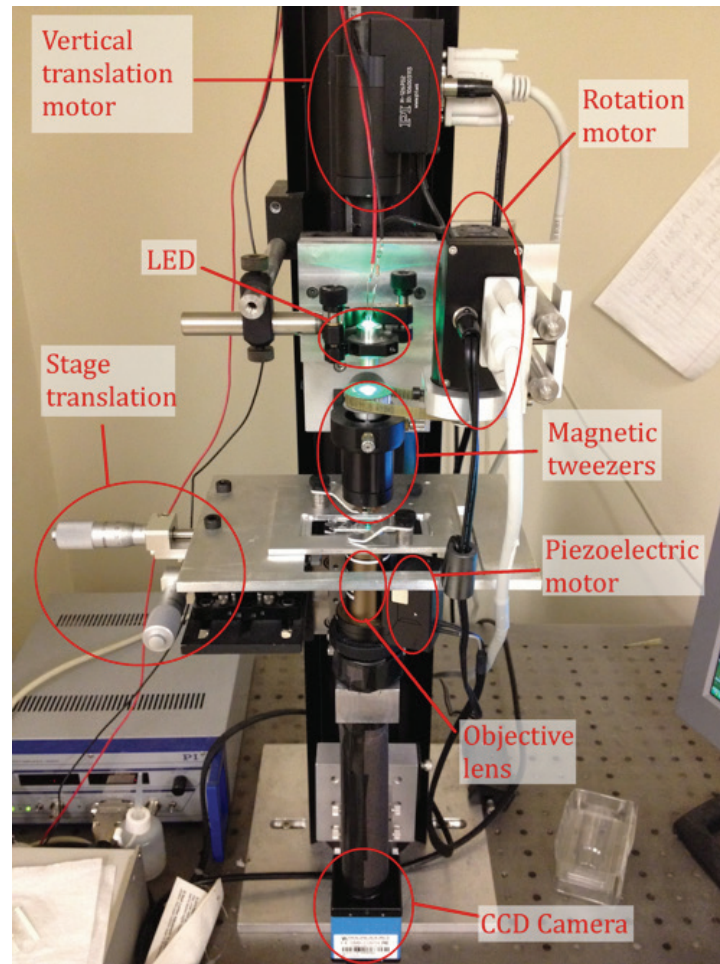


Figure 2.4: Magnetic tweezers instrument

The course adjustment of the objective lens was then used to bring the objective into contact with the immersion oil on the bottom of the chamber. The fine adjustment of the piezoelectric objective controller was set to 50 μm and the course adjustment was used to bring the beads into focus. Ordinarily, tethered beads are further from the surface, and therefore further from the focal point of the objective. This results in smaller diffraction patterns for tethered beads compared to reference beads.

To find a tether, the magnets were moved to a position corresponding to a force of $\sim 0.6-0.7$ pN (magnet position 17 mm). This force caused tethered beads to be extended to nearly their full length. The objective was adjusted so that focus was at a plane above the tethered bead. This positioning of the focus results in small diffraction patterns for tethered beads and larger diffraction patterns for reference beads. X and y translators on the stage were used to scan the chamber for usable tethers. After finding a tether, 200 μL of topo II buffer was flowed into the chamber so the DNA molecule was in the same environment that it would be when gyrase was introduced.

Before running any routines from the applet, a quick check was done on any possible tether. First, the fine focus was adjusted by one micron in either direction to see if the tether was roughly the correct length. Changing the fine focus by one micron simulates reducing the length of the tether by one micron. Given that our DNA fragment is ~ 3000 bp and 3000 bp \approx one micron, the diffraction pattern of the tethered bead *after* this change in focus should correspond to the reference bead's diffraction pattern *before* the change in focus. Following this quick length check, +20 turns were added to check for a change in DNA length. This is seen as an enlargement of the diffraction patterns around the tethered bead. After the (+) turn test, -15 turns were added. No change in length, or at least a very slight change in length, should have been seen after the addition of negative turns at a high force due to the local denaturation of DNA when unwound. After these initial checks, chapeau ("hat" in French) curves and extension vs. force curves were run for more detailed information for the specific tether in use.

2.3.1 CHAPEAU CURVES FOR EXTENSION VS. TURNS

Within the MATLAB applet is a table where parameters for acquiring chapeau curves can be entered. Chapeau curves measure the extension of the DNA molecule as a function of the number of turns added to the molecule. The name of the curve arises from the hat-like shape of this graph at low forces (Figure 2.5). In the MATLAB applet, the user can define the range of turns and the step size for a chapeau curve. For example, measurements can be taken from -30 turns to +30 turns in steps of 5 turns. The program is written so that measurements are taken from negative turns to positive turns and then back to negative turns.

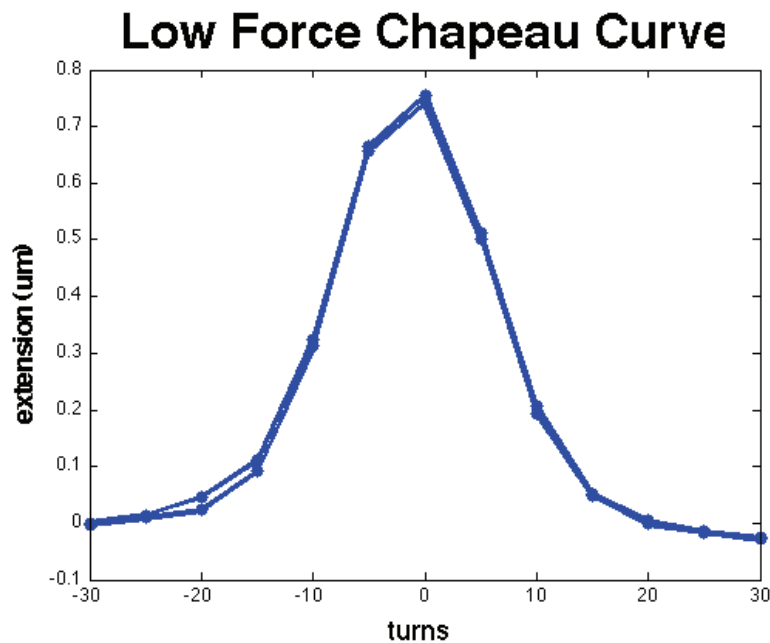


Figure 2.5: Low force chapeau curve

If the low force chapeau curve appeared uniform, then a high force chapeau curve was taken at ~ 1 pN (magnet position 17.5 mm). The purpose of the high force chapeau curve is to check that only a single DNA molecule is bound to the bead. As mentioned previously, a single DNA molecule under high tension (≥ 1 pN) will not show a decrease in length for unwinding. A typical high force chapeau curve will be taken from -15 turns to +30 turns in steps of 5. For negative turns there should be no decrease in length, but for positive turns there should be a buckling point and a subsequent decrease in length as additional turns are added (Figure 2.6).

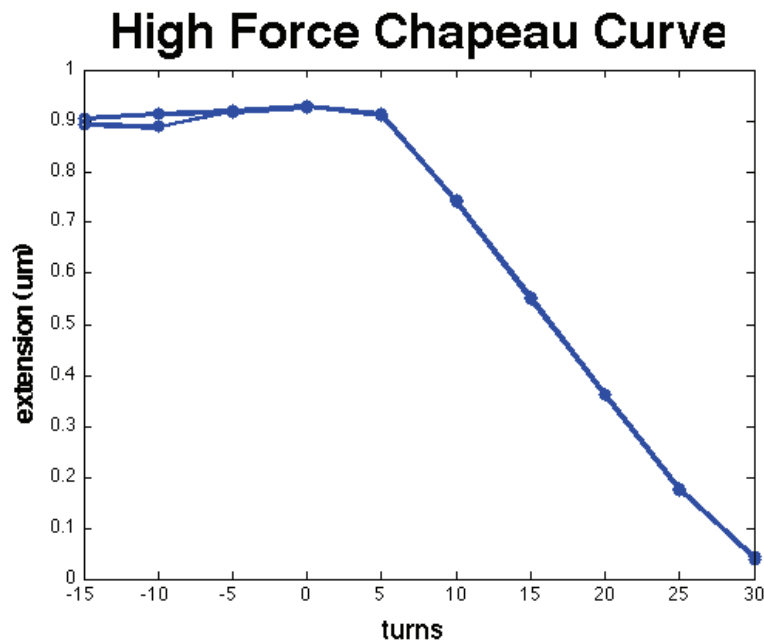


Figure 2.6: High force chapeau curve

2.3.2 FORCE VS. EXTENSION CURVES FOR FORCE VALUES

After producing the standard chapeau curves mentioned above, an extension vs. force curve was measured. The typical range for this curve is from magnet position

17.5 mm (~ 1 pN) to magnet position 14.5 mm (~ 0.1 pN) with measurements taken in steps of 0.5 mm. The purpose of this curve is to determine the corresponding force for different magnet positions.

2.3.3 DIFFERENCE IN TWO EXPERIMENT STYLES

Depending on which style of experiment was going to be run, there are two alternative directions that could be taken at this point. For the relaxation of (+) supercoils at 0.6 pN, the magnet position corresponding to 0.6 pN of force was determined from the extension vs. force measurement. Another chapeau curve at this magnet position was taken with a step size of 3 turns. As positive turns were added, a linear region could be seen where every turn added corresponded to a decrease in length. The slope of this region was used in subsequent analysis to relate a change in length to the number of turns relaxed by gyrase. Furthermore, the number of (+) turns that were mechanically added was chosen so that it fell within this linear region.

For the force modulation of gyrase activity, a low force and high force were picked from the extension vs. force measurement. A force less than 0.4 pN was considered low, while a force greater than 0.4 pN was considered high. Once these forces were chosen, higher resolution chapeau curves (step size of 2) were taken at the corresponding magnet positions. These curves were taken so that a change in length could be related to the number of turns relaxed by gyrase.

2.3.4 (+) SUPERCOIL REALAXATION EXPERIMENT

After all of these preliminary measurements were taken, *E. coli* or *Salmonella* gyrase was prepared and added to the chamber. 6 nM gyrase solutions were prepared from stocks received from Dr. Higgins (the reasoning for this concentration follows shortly). Solutions of this concentration were made using 0.4 μL of 8X diluted *E. coli* gyrase stock and 0.4 μL of 4X diluted *Salmonella* gyrase stock in 200 μL of topo II buffer with ATP. Experiments were run at both 0.2 mM and 1 mM ATP. To obtain 200 μL volumes of the desired ATP concentrations of 0.2 mM and 1 mM, 0.4 μL of 100 mM ATP stock was added to 199.6 μL of topo II buffer and 2 μL of 100 mM ATP stock was added to 198 μL of topo II buffer, respectively. After the ATP-buffer solutions were made the enzyme was added.

These solutions of ATP and enzyme in buffer were then added to the chamber. Before adjusting anything, the chamber was given a few minutes to equilibrate. After this time had passed, the force on the DNA molecule was set to 0.6 pN and the “view” function of the Matlab applet was deactivated. Deactivating the view initiates the “trace” routine. The trace function measures the extension of the tethered molecule every 0.1 seconds. The number of (+) turns determined from the linear region of the 0.6 pN chapeau curve was then added (usually 18-20 turns). The extension of the DNA molecule was monitored as the enzyme worked to relax the (+) turns introduced.

The time between the introduction of turns and the first relaxation event was termed the searching time, or lag time. This time corresponds to the time it takes for an enzyme floating freely in solution to find the supercoiled DNA molecule and

begin relaxing the supercoils. The mean searching time was used to ensure that only a single enzyme was working on each DNA molecule. A series of trials were done in which the amount of enzyme was reduced slowly while rate of relaxation was monitored. There came a point where searching times increased without any effect on relaxation time. From this range of searching times it was inferred that a single enzyme was acting on the DNA molecule. The enzyme concentration that ensured a single enzyme was working, without giving too long of a searching time, was $\sim 6\text{nM}$.

After the DNA extension returned to its original value, more (+) turns were added and the cycle was repeated for as many times as the enzyme stayed active. The number of relaxations observed fluctuated between two and six. A typical trace is shown below in Figure 2.7. A single event of enzyme activity, seen as an increase in DNA length, was called a burst. Any stopping by the enzyme between bursts, seen as an intermediate plateau, was called a pause. Pauses longer than 100 seconds, the mean searching time determined by Qing Shao in her previous work, were excluded. For pauses longer than 100 seconds, it is thought that the enzyme leaves the molecule and either the same enzyme or a new enzyme must bind to finish relaxation.

(+) Relaxation Trace

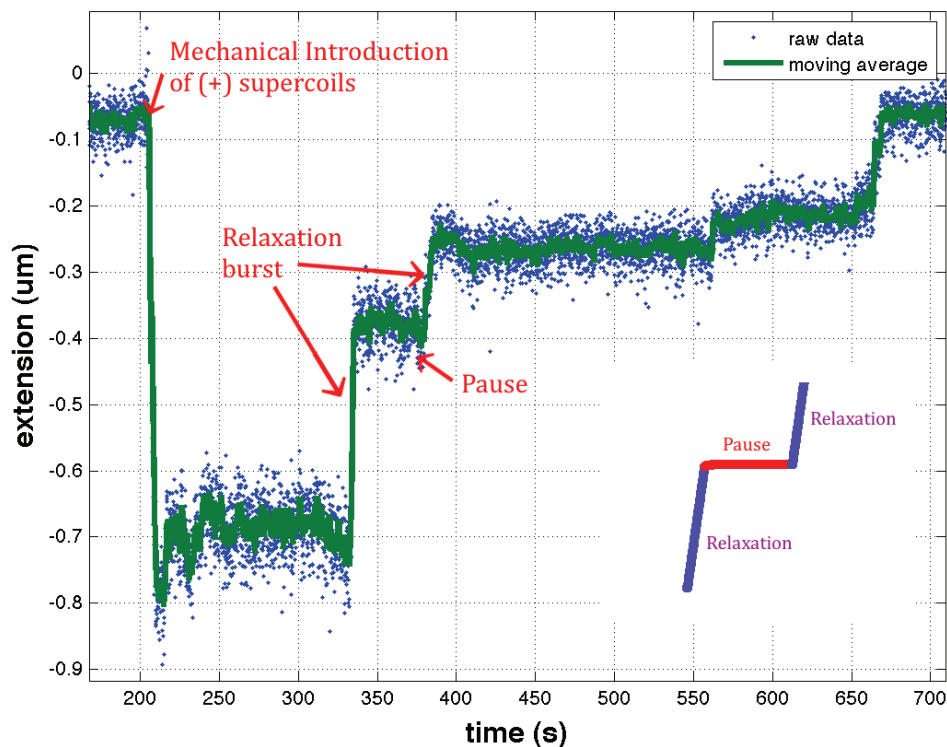


Figure 2.7: Example trace for (+) relaxation

To analyze the data, Matlab was used. Matlab's curve-fitting tool was used to calculate the slope of the linear region of the 0.6 pN chapeau curve. This value was used in a Matlab code provided by Qing Shao to calculate the rate of each burst and the length of pauses. Using a moving average with a window size of eight points, trace plots were created. The moving average line was used for selecting points that were used by the previously mentioned Matlab code to calculate rates and pauses. The codes used are attached in the appendix. A few, very minor modifications were made to Qing Shao's original codes. Comments (preceded by percentage signs) have been added to the codes for clarity.

2.3.5 FORCE MODULATION EXPERIMENT

The second style of experiment involved modulating the activity of *E. coli* and *Salmonella* gyrases by force. An enzyme concentration of 20 nM was used in Nollman's force modulation experiments [2]. This amount was verified to be the lowest concentration at which force modulation experiments could be performed. Unlike the experiments monitoring relaxation of (+) supercoils, these experiment were conducted at such a concentration that it could no longer be said that only a single enzyme was acting on the DNA. 1 mM ATP-buffer solutions were made as described previously to give a total volume of 200 μL . To this, 1.35 μL of 8X diluted *E. coli* gyrase or 0.45 μL of 2X diluted *Salmonella* gyrase was added to achieve 20 nM concentrations.

These solutions of ATP and enzyme in buffer were then added to the chamber. Before adjusting anything, the chamber was given a few minutes to equilibrate. After this time had passed, the "view" function of the Matlab applet was deactivated to begin data acquisition. The force on the DNA molecule was then set to the previously determined low force. The DNA length was monitored and the force was not changed until it was believed that the enzyme was finished *adding* supercoils. The force on the DNA molecule was then switched to the previously determined high force. Once again, DNA length was monitored and the force was not changed until it was believed that the enzyme was finished *relaxing* supercoils. This was repeated for as long as the enzyme stayed active, which was usually about five cycles.

The trace file data was analyzed using Matlab. The introduction or relaxation of supercoils by gyrase resulted in a change in extension. The higher resolution chapeau curves corresponding to each force value were used as calibration curves to convert each extension change to the number of turns introduced or relaxed. Using the time over which the extension change took place, a rate (turns/s) was calculated. Experiments were conducted for low forces ranging from 0.2-0.4 pN and high forces ranging from 0.4-0.8 pN. Additionally, experiments were conducted at a “medium” force of 0.4 pN for which *E. coli* gyrase was observed to introduce and relax (-) supercoils without user input.

3. RESULTS

3.1 (+) SUPERCOIL RELAXATION RESULTS

Traces obtained for the relaxation of (+) supercoils were to determine several parameters. First, the relaxation rate of each burst was measured. As defined in section 2.3.4, a burst is any processive relaxation event performed by gyrase. Depending on the activity of the enzyme, a burst could correspond to complete relaxation of the DNA or partial relaxation of the DNA. However, the minimum burst is two turns, which corresponds to a single enzymatic cycle. Relaxation rates for *E. coli* gyrase were compared to *Salmonella* gyrase (Figure 3.1). *Salmonella* gyrase relaxed (+) supercoils at a rate of 1.7 ± 0.9 turns/s and 2.0 ± 0.9 turns/s for 0.2mM ATP and 1.0mM ATP, respectively; *E. coli* gyrase relaxed (+) supercoils at a rate of 2.0 ± 0.8 turns/s and 2.32 ± 0.7 turns/s for 0.2mM ATP and 1.0mM ATP, respectively. *Salmonella* gyrase relaxed (+) supercoils slightly more slowly than *E. coli*, but statistically, this difference was not very significant. However, both enzymatic rates increased at higher ATP concentrations.

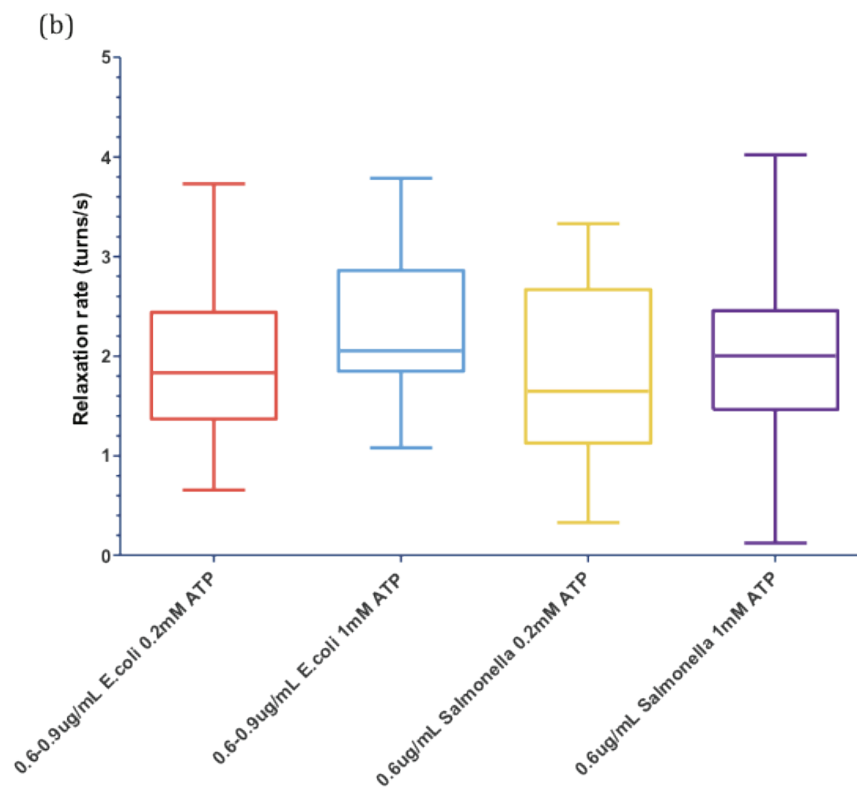
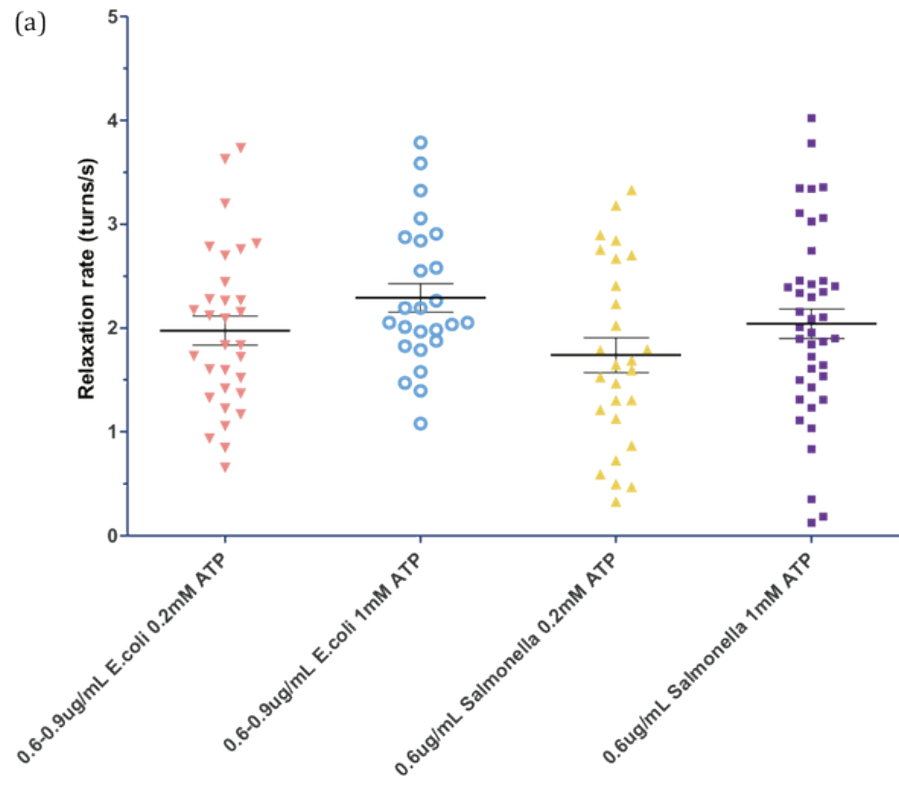


Figure 3.1: Relaxation rates for *E. coli* gyrase vs. *Salmonella* gyrase. (a) Raw data points with mean and standard deviation bars. (b) Box and whisker plots showing sample minimum, lower quartile, median, upper quartile, and sample maximum.

The number of pauses per relaxation event was analyzed (Figure 3.2). One relaxation event was defined as the time span from when gyrase first started relaxing DNA supercoils until the DNA was completely relaxed. A single relaxation event might consist of multiple bursts, and thus, multiple pauses. The number of pauses per relaxation event was measured. As discussed previously, pauses longer than 100s were not included. Both enzymes showed fewer pauses for higher ATP concentrations. However, *Salmonella* gyrase showed a higher frequency of pausing than *E. coli* gyrase for both ATP concentrations tested.

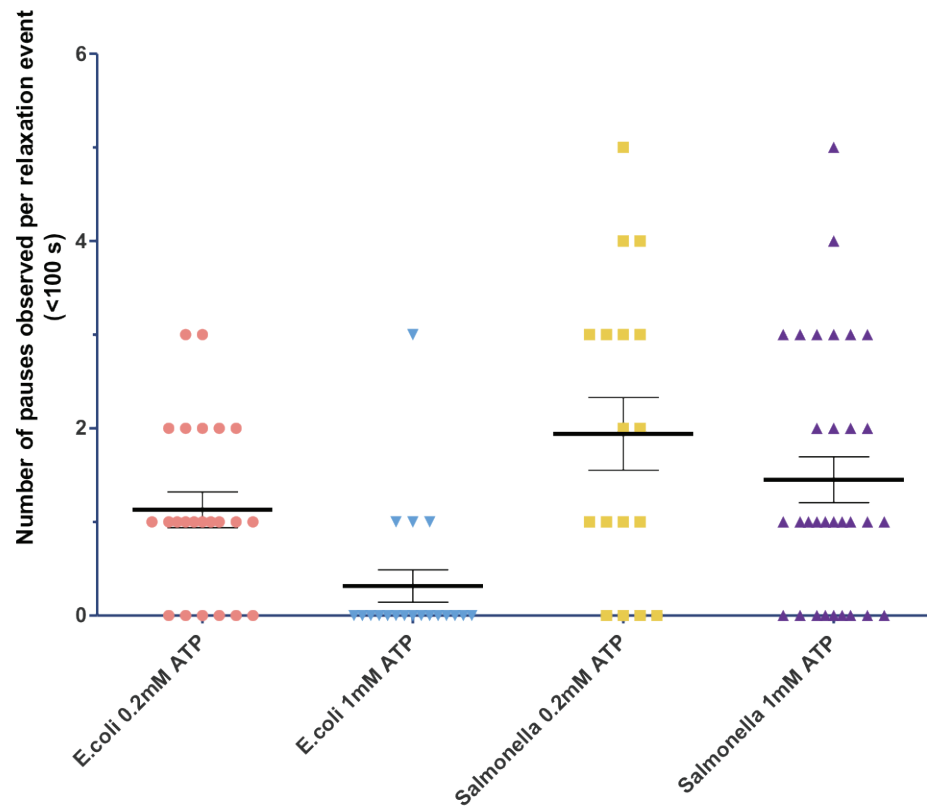


Figure 3.2: Number of pauses observed per relaxation event.

A further analysis of pausing was conducted to determine the duration of pauses. As before, pauses longer than 100s were attributed to enzyme dissociation and were excluded. *Salmonella* gyrase paused for shorter amounts of time than *E. coli* gyrase (Figure 3.3). This inverse cumulative histogram plot was created using Prism Graphpad. Combining this result with the previous result revealed that *Salmonella* gyrase paused more frequently than *E. coli* gyrase, but for slightly shorter amounts of time.

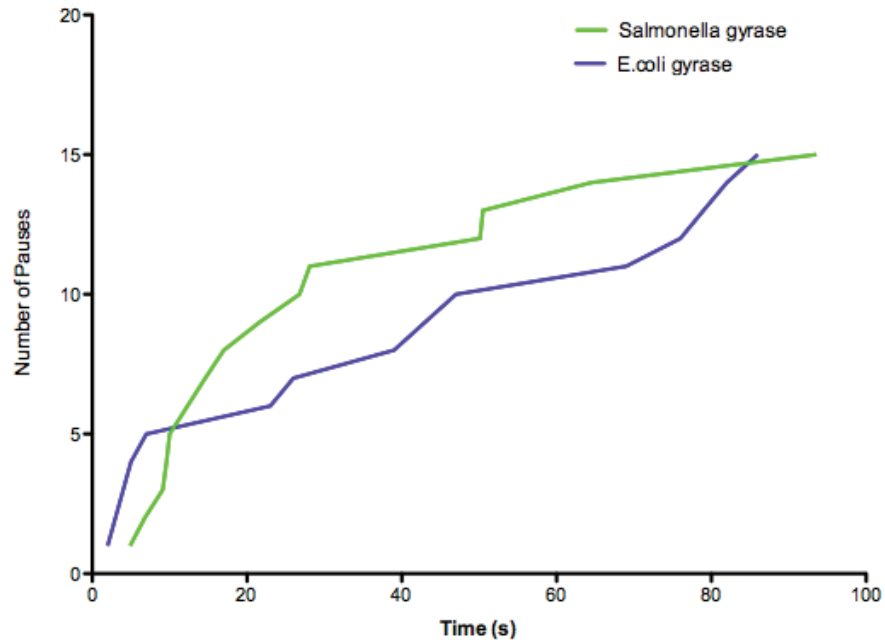


Figure 3.3: Cumulative distribution of the duration of pauses for (+) supercoil relaxation by *E. coli* and *Salmonella* gyrase

3.2 FORCE MODULATED ACTIVITY OF GYRASE

The force modulation experiments produced traces that were analyzed to determine the rates of introduction of (-) supercoils. The measured rates for the two gyrases are compared in Figure 3.4. Mean (-) supercoiling rates of 1.8 ± 0.7 turns/s and 3.0 ± 0.7 turns/s were measured for *E. coli* gyrase and *Salmonella* gyrase, respectively. Furthermore, *Salmonella* gyrase introduced a slightly larger amount of supercoils in each supercoiling event (Figure 3.5).

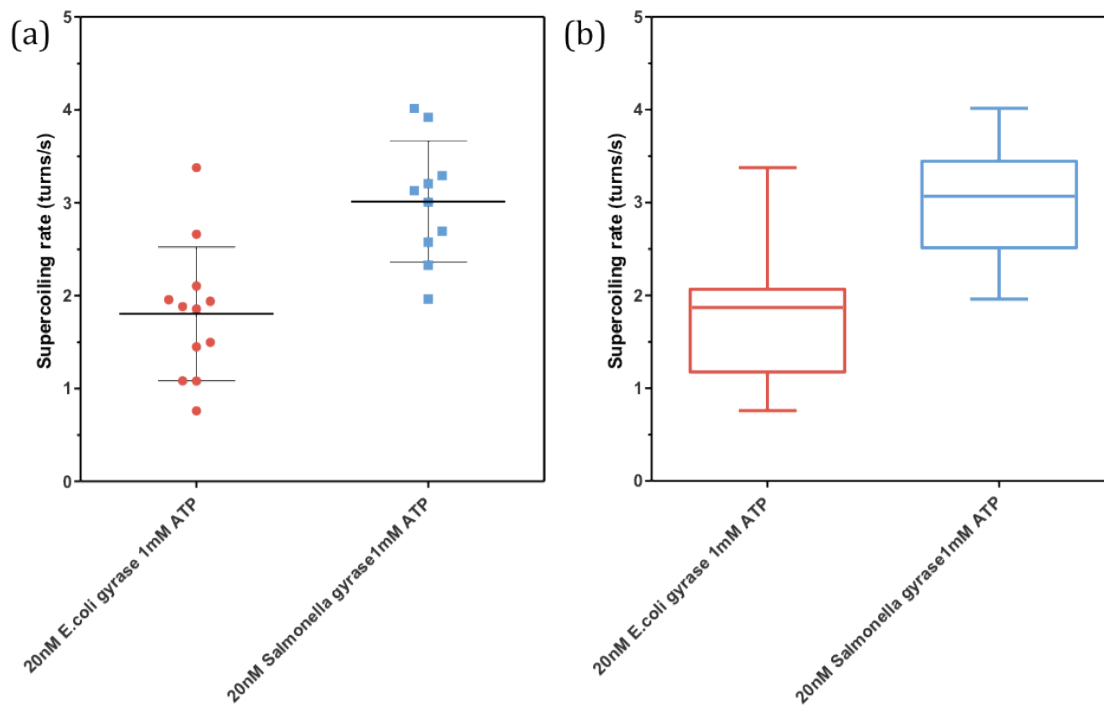


Figure 3.4: Rates of introduction of (-) supercoils by *E. coli* and *Salmonella* gyrase. (a) Raw data points with mean and standard deviation bars. (b) Box and whisker plots showing sample minimum, lower quartile, median, upper quartile, and sample maximum.

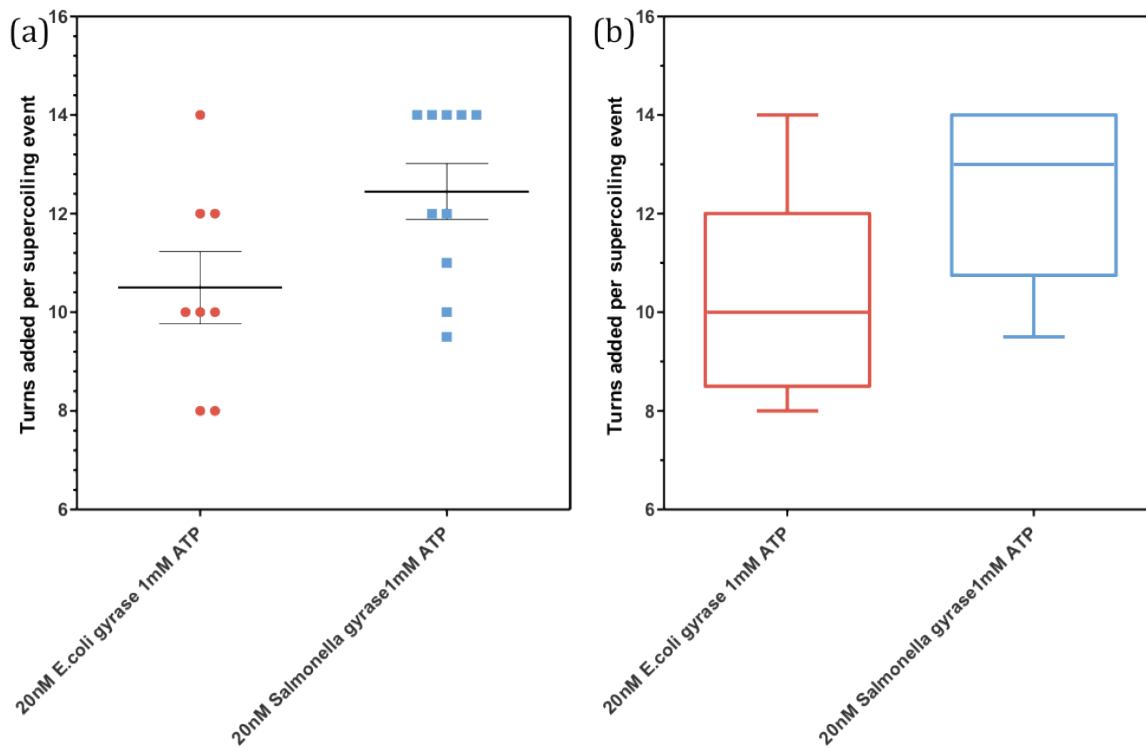


Figure 3.5: Number of (-) turns introduced by *E. coli* and *Salmonella* gyrases in each complete supercoiling event. (a) Raw data points with mean and standard deviation bars. (b) Box and whisker plots showing sample minimum, lower quartile, median, upper quartile, and sample maximum.

4. DISCUSSION

The initial hypothesis of this study was that the relative rates of (+) supercoil relaxation by *E. coli* gyrase and *Salmonella* gyrase would differ significantly. K. Champion and N. P. Higgins showed that the average supercoil density of *E. coli* is 13% higher than that of *Salmonella*. Furthermore, it was shown that during rapid growth in mid-log phase, *E. coli* was capable of generating 15% more negative supercoils than *Salmonella* [1]. Given these results, it was expected that *E. coli* gyrase would supercoil DNA at a faster rate than *Salmonella* gyrase. Furthermore, it was expected that any rate difference could be observed from the relaxation of (+) supercoils in the presence of ATP. This style of experiment was inspired by previous work performed by Qing Shao in which differences in gyrase relaxation rates were seen for DNA molecules of varying stiffness.

The relaxation of (+) supercoils by the two enzymes in the presence of ATP were much more similar than expected. As shown in Figure 3.1, *Salmonella* gyrase relaxed (+) supercoils at a slightly slower rate than *E. coli* gyrase. However, this difference may not be significant statistically. *E. coli* gyrase and *Salmonella* do, however, differ in frequency (Figure 3.2) and duration of pauses (Figure 3.3) during (+) supercoil relaxation events. *Salmonella* gyrase appears to pause more frequently, but for shorter amounts of time than *E. coli* gyrase. Thus, the processivity (-) supercoiling differs between the two gyrases.

This might be expected, since the relaxation of (+) supercoils does not require the same degree of wrapping as the introduction of (-) supercoils. Instead, the

relaxation of (+) supercoils only requires gyrase to resolve pre-existing crossovers in a plectonemic region. The DNA in this topology is in a favorable configuration for the action of gyrase. For this reason, it is not surprising that *E. coli* gyrase and *Salmonella* gyrase, which have a high degree of sequence homology, do not differ significantly in their ability to resolve crossovers in DNA that is positively supercoiled. Furthermore, topoisomerase IV is another *E. coli* topoisomerase known to relax (+) supercoils [19]. Therefore, gyrase may not be the only topoisomerase responsible for regulating positive DNA supercoiling.

The search for differences between *E. coli* gyrase and *Salmonella* gyrase continued with experiments in which the activity of gyrase in buffer containing 1mM ATP was modulated by tension. At low tensions, gyrase was able to introduce (-) supercoils; at high tensions, gyrase was able to relax (-) supercoils. Analysis of the relative rates of introduction of (-) supercoils revealed that *Salmonella* gyrase introduced supercoils faster (Figure 3.4) and to a higher degree (Figure 3.5) than *E. coli* gyrase. This result was not was expected from the findings of K. Champion and N. P. Higgins [1]. However, to investigate the origins of rate and pause differences, we next move to studying the structures and amino acid sequences of the two gyrases.

The structures and amino acid sequences of *E. coli* gyrase and *Salmonella* gyrase were analyzed in order to correlate our findings to a physical difference between the two enzymes. For *E. coli* gyrase, the amino acid sequence and crystal structure (Protein Data Bank entry: 3NUH) are available. However, for *Salmonella* gyrase, only

the amino acid sequence and models generated from this sequence are available. Unfortunately, most of these models are based on the crystal structures of *E. coli* gyrase. Due to the lack of structures to analyze, we turned to the amino acid sequence of the two enzymes.

The amino acid sequences of the two enzymes were analyzed using the UniProt Align tool. The two subunits of gyrase, *gyrA* and *gyrB*, were analyzed separately. The sequence alignment of *gyrA* and *gyrB* are shown in Figure 4.1 and Figure 4.2, respectively. The *gyrB* subunit is comprised of 804 amino acids in both *E. coli* gyrase and *Salmonella* gyrase. Of the 804 amino acids, 777 (96.6%) are identical between the two enzymes. 18 of the 27 differences occur after amino acid 568 in the C-terminal domain. However, these differences still maintain similar characteristics such as charge and polarity. Thus, the differences in amino acids might lack significance.

1	MSDLARITPVNIIEELSSYLRYAMSVIVGALPDVVDGLPVHRRVLYAMNVLGNWN	60	POAES4	GYRA_ECOLI
1	MSDLARITPVNIIEELSSYLRYAMSVIVGALPDVVDGLPVHRRVLYAMNVLGNWN	60	P37411	GYRA_SALTY
61	KAYKNSAVVGVVIGRYEPCDSAVYDITVMAQPFSLRYMLVGGQNFSGISGSSAAM	120	POAES4	GYRA_ECOLI
61	KAYKNSAVVGVVIGRYEPCDSAVYDITVMAQPFSLRYMLVGGQNFSGISGSSAAM	120	P37411	GYRA_SALTY
121	RYTEIRLAKIAEELMADLERETVDFVNYDGTETIPVMPTIPNLLVNGSSGIIVGMAT	180	POAES4	GYRA_ECOLI
121	RYTEIRLAKIAEELMADLERETVDFVNYDGTETIPVMPTIPNLLVNGSSGIIVGMAT	180	P37411	GYRA_SALTY
181	NIPPNLTVINGCLAYIDDEDISISGLMEHIPGDFPPTAALINGRRGISAYRTGRGNV	240	POAES4	GYRA_ECOLI
181	NIPPNLTVINGCLAYIDDEDISISGLMEHIPGDFPPTAALINGRRGISAYRTGRGNV	240	P37411	GYRA_SALTY
241	YIRANAEVVEADATGRRETIIVEIPYQVNAFLIKIAELVDEKRVEGISALRDESQKDG	300	POAES4	GYRA_ECOLI
241	YIRANAEVVEADATGRRETIIVEIPYQVNAFLIKIAELVDEKRVEGISALRDESQKDG	300	P37411	GYRA_SALTY
301	MIVIEVRRDAVGEVVLNLYSQTQLQVSPGINMVALHGGQKIMNLDIIIAAFVRRHRE	360	POAES4	GYRA_ECOLI
301	MIVIEVRRDAVGEVVLNLYSQTQLQVSPGINMVALHGGQKIMNLDIIISAFVRRHRE	360	P37411	GYRA_SALTY
361	VVTRRTIFELRRARDRAHILALAVLANIDPIILIRAPTPALANTALVANPWQLGNV	420	POAES4	GYRA_ECOLI
361	VVTRRTIFELRRARDRAHILALAVLANIDPIILIRAPTPALANAALISRPWBLGNV	420	P37411	GYRA_SALTY
421	AAMLERAGDDAARPEWLEPFVGRDGLYYLTQQQAAILDLQLKLTGLEHEKLLDEYKE	480	POAES4	GYRA_ECOLI
421	AAMLERAGDDAARPEWLEPFVGRDGLYYLTQQQAAILDLQLKLTGLEHEKLLDEYKE	480	P37411	GYRA_SALTY
481	LLDQIAELLHILGSARLMEVIREELLVREQFGDKRRTSITANSADINLEDLITQEDVV	540	POAES4	GYRA_ECOLI
481	LLDQIAELLHILGSARLMEVIREEMELIRDQFGERRTSITANSADINILEDLISQEDVV	540	P37411	GYRA_SALTY
541	VTLSHQGYVRYQPLSYEAQRGGGKSAARIKEDFIDRLLVANTHDTILCFSSRGVLY	600	POAES4	GYRA_ECOLI
541	VTLSHQGYVRYQPLTYEAQRGGGKSAARIKEDFIDRLLVANTHDTILCFSSRGVLY	600	P37411	GYRA_SALTY
601	SMKVYQLPEATGAGRNPIVNLPLQDEKITAILPVTEFEEGVVFMATANGTVKKTVL	660	POAES4	GYRA_ECOLI
601	WMKVYQLPEASGAGRNPIVNLPLQANERITAILPVTEFEEGVVFMATASGTVKKTAL	660	P37411	GYRA_SALTY
661	TFPNLITAGVAIKLVGDELIGVLTSGDEVMLFSAAGVVRPKESSVAMGCNTTG	720	POAES4	GYRA_ECOLI
661	TFSPHSAGIIVAVNLNGDELIGVLTSGDEVMLFSAAGVVRPKESSVAMGCNTATG	720	P37411	GYRA_SALTY
721	VKGIKLAGDDVVSLLIIPGEGAILTVTQNGYKRTAAYPTKSNATQGVISIVTERN	780	POAES4	GYRA_ECOLI
721	VKGIKLAGDDVVSLLIIPGEGAILTVTQNGYKRTAAYPTKSNATQGVISIVTERN	780	P37411	GYRA_SALTY
781	GLVVGAVQVDDCQIMMITDAGTLVTEVSEISVGNRTQGVILIRTAEDENVVGLQVVA	840	POAES4	GYRA_ECOLI
781	GSVVGAVQVDDCQIMMITDAGTLVTEVSEISVGNRTQGVILIRTAEDENVVGLQVVA	840	P37411	GYRA_SALTY
841	EPVDEEDLTIIGSAAEGDDEIAPVVDDEPEEE---	875	POAES4	GYRA_ECOLI
841	EPVDEEDLTIIGSVAEGDEIAPVVDDEPEEE---	878	P37411	GYRA_SALTY

Figure 4.1: Amino acid sequence alignment of *gyrA*. Light gray represents dissimilarities, red represents negatively charged residues, and green represents positively charged residues.



Figure 4.2: Amino acid sequence alignment of *gyrB*. Light gray represents dissimilarities, red represents negatively charged residues, and green represents positively charged residues.

The *gyrA* subunits of *E. coli* gyrase and *Salmonella* gyrase not only contain amino acid sequence differences, but they also differ slightly in length. *E. coli gyrA* is comprised of 875 amino acids, while *Salmonella gyrA* is comprised of 878 amino acids. Excluding the three extra amino acids of *Salmonella gyrA*, the remaining 875 amino acids of the *gyrA* subunit share 801 identical amino acids (91.5%). 52 of the 74 differences occur after amino acid 572 in the C-terminal domain. The three extra

amino acids of *Salmonella gyrA* are present at the C-terminus and increase this difference to 55 amino acids. These amino acid differences cause charge differences at 17 different locations. The next step was to analyze the role of these locations and the functional changes that amino acid differences might produce.

The amino acid sequences of *E. coli* gyrase and *Salmonella* gyrase differ the most in the C-terminal domains of both *gyrA*. However, the C-terminal domain of *gyrB* makes up the TOPRIM region, which is one component of the central gate. The TOPRIM region plays a role in binding and cleaving the G-segment of DNA along with the WHD of *gyrA* [13]. If one believes the idea proposed above that (+) supercoil relaxation relies primarily on the resolution of crossovers, then differences in this region could alter the rate at which (+) supercoils are relaxed. Given that the amino acid differences in this region do not change the charge or polarity of the enzyme significantly, it is not surprising that the two enzymes did not show drastic differences in (+) supercoil relaxation. However, minor rate differences could be attributed to the minor amino acid differences in the TOPRIM region.

The C-terminal domain of *gyrA* is generally referred to as the C-terminal domain of gyrase (CTD). It promotes the wrapping of DNA around gyrase in order to create an enzyme-bound positive crossover between the T- and the G-segment. It has also been proposed that the CTD can aid in the passage of the T-segment through the DNA gate and out of the C-gate [15]. Thus, the charge differences between *E. coli* gyrase's CTD and *Salmonella* gyrase's CTD could alter the gyrases' ability to wrap

DNA and produce (-) supercoils. *Salmonella* gyrase's CTD has a relative -3 charge compared to *E. coli* gyrase's CTD. This could decrease *Salmonella's* ability to bind DNA compared to *E. coli* gyrase. This decreased ability to hold DNA could explain the higher rate of pausing observed by *Salmonella* gyrase (Figure 3.2).

The force-modulated style of experiment used to collect (-) supercoil data is a relatively recent undertaking and more data is being accumulated for this portion of the study at the time of writing. The force-modulated data presented in this thesis includes a low number of data points due to the small amount of experiments run thus far. However, further investigation is planned in order to verify the trends observed.

5. CONCLUSION

Eukaryotic and prokaryotic organisms possess members of the topoisomerase family of enzymes in order to regulate the level of DNA supercoiling throughout their life cycle. DNA supercoiling is regulated in a dynamic fashion and is known to play a role in the expression of genes, site-specific recombination, DNA condensation, and the segregation of chromosomes [9]. K. Champion and N. P. showed that switching the gyrases of *E. coli* and *Salmonella* resulted in death of the bacteria [1]. The goal of this study was to explore the differences between *E. coli* gyrase and *Salmonella* gyrase using single molecule experiments. Magnetic tweezers were used to investigate the relative relaxation rates of (+) and (-) supercoils, frequency of pausing, and duration of pausing.

It was found that *E. coli* gyrase and *Salmonella* gyrase relaxed (+) supercoils at statistically similar rates. The slightly faster rate of *E. coli* gyrase, may result from the slight differences in the amino acid sequence of the TOPRIM regions of the two gyrases. Pausing was excluded from this measurement and thus this difference does not reflect the fact that *Salmonella* gyrase was also observed to pause for shorter durations, but at a higher frequency than *E. coli* gyrase.

Salmonella gyrase also relaxed (-) supercoils faster than *E. coli* gyrase. Mean (-) supercoiling rates of 1.8 ± 0.7 turns/s and 3.0 ± 0.7 turns/s were measured for *E. coli* gyrase and *Salmonella* gyrase, respectively. Additionally, *Salmonella* gyrase introduced a slightly larger number of supercoils in each supercoiling event. This portion of the study, however, is a relatively new undertaking and only the initial

data is presented here. More data needs to be collected for a more comprehensive analysis of (-) supercoiling by *E. coli* and *Salmonella* gyrase.

Future areas of investigation will include further (-) supercoil experiments, wrapping experiments, gyrase cofactors, and possibly studies with gyrase cofactors and mutants. First, for a more detailed analysis of (-) supercoil relaxation rates of *E. coli* gyrase and *Salmonella* gyrase, more force-modulated experiments and “medium” force experiments need to be run. Second, wrapping experiments can be conducted to investigate differences between *E. coli* *gyrA* CTD and *Salmonella* *gyrA* CTD. A wrapping experiment monitors DNA extension in the presence of gyrase without ATP. Third, a literature search for and possibly experiments with gyrase cofactors could shed additional light on differences between the two enzymes. Last, gyrase mutants with mutated *gyrA* or *gyrB* subunits could be used to pinpoint the location of enzyme differences.

APPENDIX

A1 PLOT TRACE FILE

```

clear all;
% import the trace file
A=importdata('trace.txt');
% subtract the reference bead extension from the tethered bead
extension
A(:,8)=A(:,7)-A(:,4);
B=A;
% correct the time to start at zero seconds
B(:,1)=B(:,1)-B(1,1);
% apply moving average of 10
[ShortA,LongA]= movavg(B(:,8),10,80);
% plot moving average and raw data points
plot( B(:,1),B(:,8),'.',B(:,1),ShortA,'LineWidth',3);
% label graph
hold on;
ylabel('extension (um)','fontsize',15,'fontweight','b');
xlabel ('time (s)','fontsize',15,'fontweight','b');
title ('(+) Relaxation Trace','fontsize',25,'fontweight','b');
grid on
hold off;
legend('raw data','moving average');

```

A2 RATE CALIBRATION

```

% fact = slope of linear region of 0.6 pN chapeau curve
fact=0.037;
% crosshairs for selection of beginning and end of burst
[x,y]=ginput(2);
% time in x-direction
t=x(2)-x(1)
% extension in y-direction
z=y(2)-y(1)
% change in turns = change in extension / slope of chapeau
turn=z/fact
% rate = change in turns / change in time
r=turn/t

```

BIBLIOGRAPHY

1. Champion, K. and N.P. Higgins, *Growth rate toxicity phenotypes and homeostatic supercoil control differentiate Escherichia coli from Salmonella enterica serovar Typhimurium*. J Bacteriol, 2007. **189**(16): p. 5839-49.
2. Nollmann, M., et al., *Multiple modes of Escherichia coli DNA gyrase activity revealed by force and torque*. Nat Struct Mol Biol, 2007. **14**(4): p. 264-71.
3. Lehninger, A.L., D.L. Nelson, and M.M. Cox, *Lehninger principles of biochemistry*. 5th ed2008, New York: W.H. Freeman.
4. Watson, J.D. and F.H.C. Crick, *Molecular structure of nucleic acids: a structure for deoxyribose nucleic acid*. Nature, 1953. **171**(4356): p. 737-8.
5. Von Hippel, P.H. and J.D. McGhee, *DNA-protein interactions*. Annu Rev Biochem, 1972. **41**(10): p. 231-300.
6. Boles, T.C., J.H. White, and N.R. Cozzarelli, *Structure of plectonemically supercoiled DNA*. J Mol Biol, 1990. **213**(4): p. 931-51.
7. Strick, T.R., et al., *Behavior of supercoiled DNA*. Biophys J, 1998. **74**(4): p. 2016-28.
8. Wang, J.C., *Cellular roles of DNA topoisomerases: a molecular perspective*. Nat Rev Mol Cell Biol, 2002. **3**(6): p. 430-40.
9. Zechiedrich, E.L., et al., *Roles of topoisomerases in maintaining steady-state DNA supercoiling in Escherichia coli*. J Biol Chem, 2000. **275**(11): p. 8103-13.
10. Schoeffler, A.J., A.P. May, and J.M. Berger, *A domain insertion in Escherichia coli GyrB adopts a novel fold that plays a critical role in gyrase function*. Nucleic Acids Res, 2010. **38**(21): p. 7830-44.
11. Schoeffler, A.J. and J.M. Berger, *Recent advances in understanding structure-function relationships in the type II topoisomerase mechanism*. Biochem Soc Trans, 2005. **33**(Pt 6): p. 1465-70.
12. Corbett, K.D. and J.M. Berger, *Structure, molecular mechanisms, and evolutionary relationships in DNA topoisomerases*. Annu Rev Biophys Biomol Struct, 2004. **33**: p. 95-118.
13. Schoeffler, A.J. and J.M. Berger, *DNA topoisomerases: harnessing and constraining energy to govern chromosome topology*. Q Rev Biophys, 2008. **41**(1): p. 41-101.
14. Ruthenburg, A.J., et al., *A superhelical spiral in the Escherichia coli DNA gyrase A C-terminal domain imparts unidirectional supercoiling bias*. J Biol Chem, 2005. **280**(28): p. 26177-84.
15. Baker, N.M., et al., *Solution structures of DNA-bound gyrase*. Nucleic Acids Res, 2011. **39**(2): p. 755-66.
16. Neuman, K.C. and A. Nagy, *Single-molecule force spectroscopy: optical tweezers, magnetic tweezers and atomic force microscopy*. Nat Methods, 2008. **5**(6): p. 491-505.
17. Koster, D.A., et al., *Cellular strategies for regulating DNA supercoiling: a single-molecule perspective*. Cell, 2010. **142**(4): p. 519-30.

18. Gore, J., et al., *Mechanochemical analysis of DNA gyrase using rotor bead tracking*. *Nature*, 2006. **439**(7072): p. 100-4.
19. Peter, B.J., et al., *Genomic transcriptional response to loss of chromosomal supercoiling in Escherichia coli*. *Genome Biol*, 2004. **5**(11): p. R87.